

Nanoscale

Accepted Manuscript



This is an *Accepted Manuscript*, which has been through the Royal Society of Chemistry peer review process and has been accepted for publication.

Accepted Manuscripts are published online shortly after acceptance, before technical editing, formatting and proof reading. Using this free service, authors can make their results available to the community, in citable form, before we publish the edited article. We will replace this *Accepted Manuscript* with the edited and formatted *Advance Article* as soon as it is available.

You can find more information about *Accepted Manuscripts* in the [Information for Authors](#).

Please note that technical editing may introduce minor changes to the text and/or graphics, which may alter content. The journal's standard [Terms & Conditions](#) and the [Ethical guidelines](#) still apply. In no event shall the Royal Society of Chemistry be held responsible for any errors or omissions in this *Accepted Manuscript* or any consequences arising from the use of any information it contains.

COMMUNICATION

Low affinity binding of plasma proteins to lipid-coated quantum dots as observed by in-situ fluorescence correlation spectroscopy

Cite this: DOI: 10.1039/x0xx00000x

Received 00th January 2012,
Accepted 00th January 2012

DOI: 10.1039/x0xx00000x

www.rsc.org/

Yvonne Klapper,^a Pauline Maffre,^a Li Shang,^a Kristina N. Ekdahl,^{b,c} Bo Nilsson,^c Simon Hettler,^d Manuel Dries,^d Dagmar Gerthsen^d and G. Ulrich Nienhaus,^{a,e,f,*}

Protein association to lipid-coated nanoparticles has been pursued quantitatively by using fluorescence correlation spectroscopy. For three important plasma proteins, we found extremely low binding affinities toward lipid-enwrapped quantum dots (QDs). The apparent equilibrium dissociation coefficients were in the range of several hundred micromolar; orders of magnitude lower than for binding to QDs coated by dihydrolipoic acid.

The study of engineered nanomaterials interacting with biological systems is presently a most exciting research topic at the interface between nanotechnology and the life sciences.¹⁻³ It is now well established that nanoparticles (NPs) encountering biological fluids are swiftly coated by a biomolecular adsorption layer, the so-called "protein corona".^{4, 5} Consequently, the molecular machinery of a living cell or organism will – at least initially – interact with the corona rather than the bare NP, making it a key determinant of the biological response of NP exposure.⁶ Indeed, studies have reported that protein adsorption onto NPs affects their cellular uptake efficiency, controls the internalization mechanism,⁷ and modulates pathobiological effects.⁸ Therefore, a profound knowledge of the protein corona, including its composition, structure, dynamics and thermodynamics, is of fundamental importance for the safe and well controlled application of NPs.

Recent studies have revealed that different factors affect the interactions between NPs and proteins.^{9, 10} Surface properties of NPs, especially, surface chemical functionality and electrostatic potential, play an essential role. For example, NP surfaces with neutral charge have been reported to show a reduced tendency to bind proteins than their negatively charged (COOH functionalized) or positively charged (NH₂ functionalized) counterparts.¹¹ Polyethylene glycol (PEG) functionalization can also reduce protein adsorption onto NP surfaces.¹² Other surface modifications such as carboxyl and citrate induce monolayer corona formation.¹³

Here we present a quantitative study of protein corona formation on lipid-coated NPs (lipid-NPs), an important type of nanomaterials that have been widely used as vehicles for drug delivery, owing to their good biocompatibility, long retention time in the blood circulation, and facile controllability.^{14, 15} Currently, a quantitative understanding of protein adsorption onto lipid-coated NP surfaces at

the molecular level is still largely missing.¹⁶ Such knowledge would not only be beneficial for the further development of efficient lipid-based drug vehicles, but would also contribute to our general understanding of surface effects regulating protein-NP interactions. Herein, we applied fluorescence correlation spectroscopy (FCS) to simultaneously determine binding affinities of proteins to NPs and the thickness of the protein adsorption layer. Unlike the majority of other approaches requiring purification of NP-protein complexes from unbound protein prior to the analysis, FCS allows a quantitative *in situ* observation of protein adsorption, i.e., while the proteins are present in the fluid.¹⁷ This unique feature is very important since it closely resembles the situation in the biological environment.

Luminescent semiconductor quantum dots (QDs) are among the most widely used engineered NPs, therefore, we adopted them as model particles. Lipid-coated QDs were prepared via a simple lipid wrapping approach using myristoyl-hydroxyl-phosphatidylcholine (MHPC) lipids and stearic acid (molar ratio 3.2:1; for details, see Experimental Section in ESI).¹⁸ The obtained lipid-QDs displayed good dispersity in aqueous solution, with a ζ -potential of -9.3 ± 0.5 mV, attributed to zwitterionic head group of lipids. These lipid-QDs feature a strong fluorescence with the emission maximum at 606 nm (Figure 1A). High-resolution transmission electron microscopy (HRTEM) revealed an average core diameter of (5.2 ± 0.8) nm (Figure 1B), whereas the hydrodynamic diameter was (13.6 ± 1.8) nm, as measured by dynamic light scattering (DLS) in aqueous solvent. The lipid layer around the QD surfaces was also visualized by HRTEM using osmium staining, yielding an increase in diameter in the expected range, i.e., ~ 1.0 nm (Figure S1).

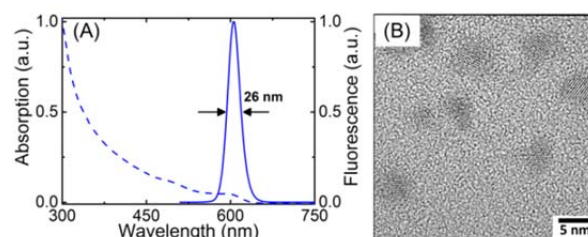


Figure 1. (A) Absorption (dashed line) and fluorescence emission (solid line) spectra of lipid-QDs in PBS; (B) typical TEM image of lipid-QDs.

We chose three important plasma proteins for our study: human plasma albumin (HSA), apolipoprotein E3 (ApoE3) and complement component 3 (C3). HSA is the most abundant protein in human blood plasma and a carrier of many poorly water-soluble small molecules. ApoE3 is an important transporter of lipids in blood by forming water-soluble lipoproteins. C3 is the central component of the complement system which is central in innate immunity, and which is responsible for inflammatory response.^{19, 20} An increase of the hydrodynamic radius of lipid-QDs, was observed when mixing with increasing concentrations of all three proteins in PBS, indicating clearly the formation of a protein corona (Figure 2). Interestingly, in contrast to our previous studies of NP-protein interactions,^{13, 21, 22} saturation was not reached for the three proteins adsorbing onto lipid-QDs within the accessible concentration range (for ApoE3 and C3, we note that the highest possible concentrations were *ca.* 30 μM due to solubility limitations), indicating a very low binding affinity. Especially for ApoE3, the size increase was only noticeable for protein concentrations above 10 μM . In support of the very weak binding, the photophysical properties (i.e., fluorescence intensity and lifetime) of the lipid-QDs also did not show any measurable changes at low ApoE3 concentration (data not shown), which would be expected upon protein association.^{23, 24}

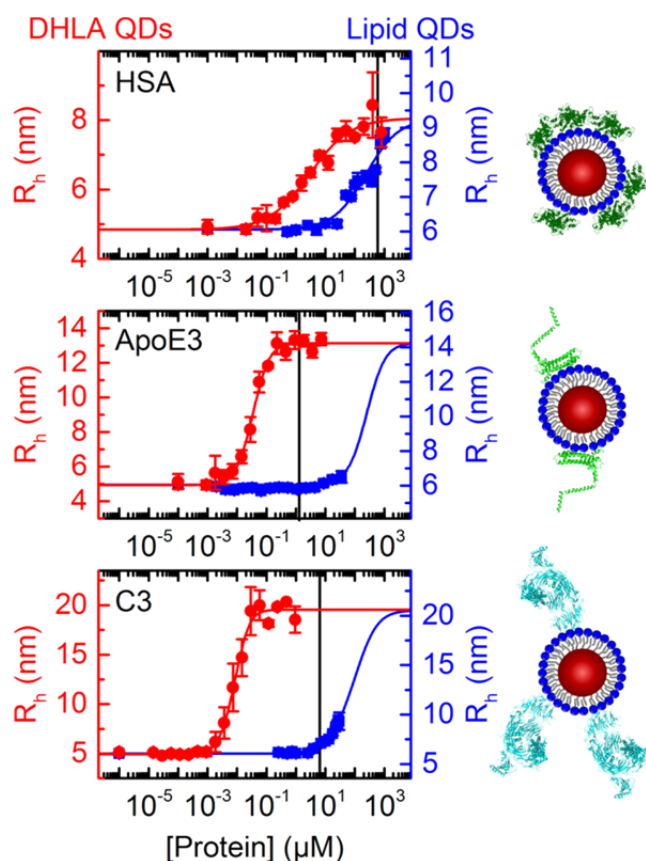


Figure 2. Hydrodynamic radius of DHLA-QDs (red curves, red axis on the left) and lipid-QDs (blue curves, blue axis on the right) measured by 2fFCS (dots) and fitted as described (lines), as a function of the concentration of HSA, ApoE3 and C3. The black vertical lines in the graphs indicate their typical concentrations in blood. On the right hand side of the graphs, lipid QDs with bound protein are depicted as they may look like at the highest protein concentrations employed.

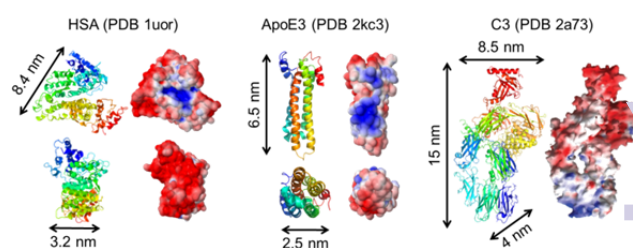


Figure 3. Molecular depictions of HSA, ApoE3 and C3, showing their tertiary structures (cartoons) with their overall dimensions as measured with Pymol based on the corresponding PDB files (1our for HSA, 2kc3 for the N-terminal domain of ApoE3, 2a73 for C3), as well as their electrostatic potential. The potentials of HSA and ApoE3 were calculated online by using the PDB2PQR server (http://nbc-222.ucsd.edu/pdb2pqr_1.9.0/) at a pH of 7.4. The red (blue) areas correspond to a negative (positive) potential. The display range is from $-5 k_B T/e$ to $5 k_B T/e$. For C3, the electrostatic potential image (display range $-12 k_B T/e$ to $12 k_B T/e$) was taken from the literature.²⁵

For comparison, we studied protein binding to QDs coated with dihydroliipoic acid (DHLA-QDs). Their spectroscopic characterization is shown in Figure S2.²⁶ These NPs had identical cores as the lipid-QDs but different surface functionalization, i.e., carboxylic acid surface ligands, leading to a lower ζ -potential (-25 ± 2) mV. In comparison with lipid-QDs, the radius increase of DHLA-QDs upon protein adsorption happened at much lower protein concentrations; complete saturation was achieved in all the cases, clearly revealing a much higher affinity of these proteins for DHLA-QDs than for lipid-QDs. By quantitative analysis of the NP radius increase as a function of the protein concentration,¹³ we obtained much smaller dissociation coefficients (K'_D) for DHLA-QDs than lipid-QDs (results are summarized in Table 1). For HSA, K'_D for DHLA-QDs ($6.4 \pm 3.6 \mu\text{M}$) is ~ 100 fold lower than that for lipid-QDs ($400 \pm 70 \mu\text{M}$). Our quantitative analysis also gives the Hill coefficient, n , a measure of NP-protein binding cooperativity. For the binding of HSA, n was below 1 (anti-cooperativity), as observed before, whereas for ApoE3 and C3, n was above 1 (cooperativity).

To obtain a converging fit for the data of lipid-QDs in the absence of saturation, we had to keep the radius increase identical for a particular protein binding to DHLA- as well as lipid-QDs. This can be done in the analysis by holding N_{max} , the maximum number of proteins binding at saturation, fixed. The rationale behind this was that both types of QDs carry charged ligands and are overall negatively charged. In such cases, we have found that the specific orientation of the protein molecules on the QD surface is mainly governed by charge interactions,^{22, 26, 27} so that we expect a similar or even identical corona thickness for both NPs. We note that the absolute number of N_{max} must be taken with caution. In our standard analysis, we assume that the volume of the protein corona (i.e., the volume of the spherical shell with radius $R_h(0)$ and thickness ΔR_h) is completely taken up by proteins. However, dense packing of proteins may be difficult to achieve, depending on the size or shape of the protein forming the monolayer, and free space between the proteins may be taken up by solvent molecules. Alternatively, we may estimate N_{max} by dividing the surface area of the bare QD by the footprint of the protein, i.e., the face with which the protein molecule presumably attaches to the QDs (Table 1).

Furthermore, the maximum radius increase (ΔR_h) gives us important clues about the orientation of the proteins relative to the NP surfaces. For HSA, $\Delta R_h = (3.3 \pm 0.6)$ nm, indicating that HSA molecules form a monolayer around the QDs. The structure of HSA can be approximated as a 3.2 nm thick triangular prism with sides of

Table 1. Binding parameters obtained from fitting the data shown in Figure 2 using the Hill equation. ΔR_h is the maximum hydrodynamic radius increase of the QDs observed due to protein adsorption, K_D is the midpoint concentration of the transition and n is the Hill coefficient. N_{max} is the maximum number of protein molecules bound, assuming that the entire added volume is taken up by proteins (volume model) or, alternatively, that proteins adsorb with specific footprints on the surface (surface model).

	HSA		ApoE3		C3	
	DHLA-QDs	Lipid-QDs	DHLA-QDs	Lipid-QDs	DHLA-QDs	Lipid-QDs
ΔR_h (nm)	3.3 ± 0.6	3.3^a	8.2 ± 0.3	8.2^a	14.6 ± 0.2	14.6^a
K_D (μM)	6.4 ± 3.6	400 ± 70	0.06 ± 0.01	430 ± 120	0.015 ± 0.001	210 ± 30
n	0.8 ± 0.1	0.7 ± 0.2	1.7 ± 0.2	1.5 ± 0.2	2.1 ± 0.2	1.3 ± 0.1
N_{max}^b	18 ± 2	26^a	72 ± 4	90^a	60 ± 2	71^a
N_{max}^c	9.5 ± 0.8	15 ± 2	19 ± 1	28 ± 1	8.9 ± 0.4	14 ± 2

^{a)} parameters fixed in the fit by choosing N_{max} to yield the same ΔR_h as for DHLA-QDs in the fit.

^{b)} calculated by the volume model

^{c)} calculated by the surface model

8.4 nm (Figure 3), thus, the HSA molecules are likely to bind to the QD surface with one of their triangular faces.^{13, 22} This view is further supported by the fact that a big patch with positive electrostatic potential is present on one of these faces (Figure 3), which then favors binding to the negatively charged groups on both DHLA-QDs and lipid-QDs *via* electrostatic interactions.

For ApoE3, a fairly large radius increase of (8.2 ± 0.3) nm was obtained upon adsorption onto our QD surfaces, which is slightly larger than the radius increase we observed for a similar apolipoprotein, ApoE4, on polymer-coated FePt NP surfaces where we measured (5.7 ± 0.2) nm.²² The structure of ApoE4 consists of a four-helix bundle resembling a cylinder of 6–7 nm in height and 2–3 nm in width. Two more helices are connected at the C-terminal part; their crystal structure is still not resolved.²⁸ There is a large patch with a positive electrostatic potential along the four-helix bundle, through which the interaction with the negatively charged surface likely occurs. ApoE3 possesses a similar positive patch (Figure 3), through which the interaction with the DHLA-QDs probably occurs. It was shown that the presence of an arginine at position 112 in ApoE4 helps stabilizing one of the two helices at the C-terminus, resulting in a more compact structure, whereas in ApoE3, the two helices may move more freely in solution, thus yielding a larger radius increase.²⁹ Note that the higher affinity of ApoE3 for DHLA-QDs with respect to HSA (Table 1) may be a consequence of the larger positive patch on the surface of ApoE3 than HSA, as we had proposed earlier for HSA and ApoE4 binding to polymer-coated NPs.²²

Similar as with ApoE3, no saturation could be reached with C3 on lipid-QDs in our experiments for concentrations up to 30 μM . By contrast, for DHLA-QDs, complete saturation was obtained, yielding a radius increase of (14.6 ± 0.2) nm. This value can again be rationalized with the dimensions and the charge distribution of C3: the C3 protein molecule folds into an elongated structure, with dimensions of about 4.0 nm \times 8.5 nm \times 15 nm (Figure 3). The electrostatic potential map of C3 also reveals a positive patch at the 4.0 nm \times 8.5 nm edge. Thus, one should expect binding of the C3 molecule to the negatively charged QD through this big positive patch, leading to a radius increase of about 15 nm. The fitted apparent dissociation coefficient was 0.015 ± 0.001 μM and 210 ± 30 μM for the DHLA-QDs and lipid-QDs, respectively. This difference of a factor $\sim 10\,000$ reveals, as for HSA and ApoE3, a much weaker interaction of the C3 protein with the lipid-QDs.

In Figure 2, the black vertical lines indicate the typical protein concentration in plasma for healthy individuals (HSA: ~ 40 g/l,³⁰ *i.e.*, ~ 600 μM , ApoE3: ~ 0.045 g/l,³¹ *i.e.*, 1.3 μM , C3: ~ 1.2 g/l,²⁵ *i.e.*,

~ 6.4 μM). Thus, if DHLA-QDs were present in the blood flow in a small concentration, HSA, ApoE3 or C3 would all have the tendency to complete overcoat them. By contrast, only HSA would partially adhere to the surface of lipid-QDs. The extremely low tendency of lipid-QDs to adsorb plasma proteins is likely a consequence of the zwitterionic nature of their lipid coating. Previous studies have already shown that zwitterionic monolayers³² as well as neutral surfaces (*e.g.*, PEG functionalization)³³ can efficiently resist non-specific protein adsorption. Both kinds of surfaces are well hydrated and have low net charge, which together result in only weak interactions with dissolved species such as proteins.³⁴ In the lipid wrapped QD constructs, the heads of the lipid molecules end on lipid-QD surfaces with less charges in physiological environment (pH 7.4), but still sufficient for good dispersity. Lipid-QDs indeed possess less surface charge than carboxylate-coated QDs in PBS, as inferred from the ζ -potential measurements. Moreover, for lipid nano-emulsions, it is known that lipid particle-protein interactions may give rise to significant conformational changes of both proteins and emulsion particles (*i.e.*, formation of a protein-particle complex with its own structure).²⁹ The fact that the lipid molecules in our QDs are grafted as a monolayer to a rigid core may prevent such a structural rearrangement and thus suppress interactions between the hydrophobic lipid tails and the proteins.

In summary, we have presented a first quantitative investigation of the adsorption of blood plasma proteins onto lipid-coated QDs by using FCS. This method allows us to measure protein binding *in situ*, *i.e.*, in a protein-containing solution in equilibrium, by determining the average hydrodynamic radius of the NP-protein complexes; it thus directly reveals the thickness of the protein layer. Strikingly, the plasma proteins studied here all exhibited extremely low binding affinities toward lipid-coated QDs, orders of magnitude lower than toward DHLA-coated QDs. Also in comparison with other NPs (*i.e.*, polymer-coated FePt NPs,²² D-penicillamine-coated QDs³⁵), the binding affinity of lipid-QDs was much reduced. The weak protein adhesion tendency makes lipid-coated NPs attractive for biotechnology applications, *e.g.*, as drug nanocarriers, for which the suppression of non-specific protein adsorption is important to achieve highly efficient targeted delivery. Furthermore, the absolute size increase was found to be correlated with the molecular dimensions of adsorbed proteins, in agreement with previous reports.^{22,26,35} The findings presented here underscore the importance of NP surface properties for defining their biological interactions and complement our knowledge about protein adsorption onto NPs in a significant way. Finally, we note that interactions of plasma proteins with lipid coatings are likely to vary with the nature of the lipid

molecules as well as with the curvature of NP core. Therefore, more research will be desirable to further advance our understanding of interactions between lipidic NP surfaces and proteins at the nanoscale.

Acknowledgements

This work was supported by the KIT within the context of the Helmholtz Program STN, by grant 2013-65X-05647-34-4 from the Swedish Research Council (VR), and from the AFA Insurance. AFA is a nonprofit insurance company that is jointly owned by the Swedish Labor Organization and the Swedish Employers Organization. Y. K. acknowledges a fellowship from the Karlsruhe School of Optics and Photonics (KSOP), L. S. is supported by the Carl-Zeiss-Stiftung.

Notes and references

^a Institute of Applied Physics and Center for Functional Nanostructures, Karlsruhe Institute of Technology (KIT), Karlsruhe, Germany. E-mail:

uli@illinois.edu

^b Linnæus Center of Biomaterials Chemistry, Linnæus University, Kalmar, Sweden

^c Department of Immunology, Genetics and Pathology, Uppsala University, Uppsala, Sweden

^d Laboratory of Electron Microscopy (LEM), KIT, Karlsruhe, Germany

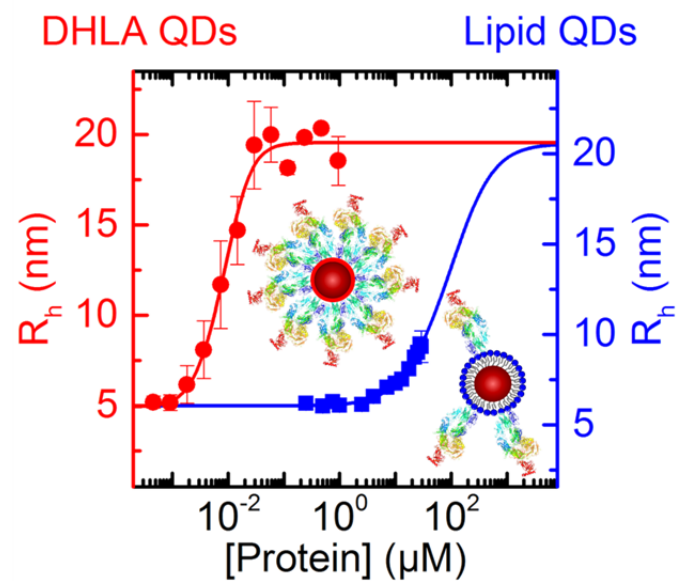
^e Institute of Toxicology and Genetics, KIT, Eggenstein-Leopoldshafen, Germany

^f Department of Physics, University of Illinois at Urbana-Champaign, Illinois, USA

Electronic Supplementary Information (ESI) available: [Experimental details and Figures S1-S3]. See DOI: 10.1039/c000000x/

- W. J. Stark, *Angew. Chem. Int. Ed.*, 2011, 50, 1242-1258.
- L.-C. Cheng, X. Jiang, J. Wang, C. Chen and R.-S. Liu, *Nanoscale*, 2013, 5, 3547-3569.
- B. Pelaz, G. Charron, C. Pfeiffer, Y. Zhao, J. M. de la Fuente, X.-J. Liang, W. J. Parak and P. del Pino, *Small*, 2013, 9, 1573-1584.
- T. Cedervall, I. Lynch, S. Lindman, T. Berggård, E. Thulin, H. Nilsson, K. A. Dawson and S. Linse, *Proc. Natl. Acad. Sci. USA*, 2007, 104, 2050-2055.
- P. d. Pino, B. Pelaz, Q. Zhang, P. Maffre, G. U. Nienhaus and W. J. Parak, *Mater. Horizons*, 2014, 1, 301-313.
- M. P. Monopoli, C. Aberg, A. Salvati and K. A. Dawson, *Nat. Nanotechnol.*, 2012, 7, 779-786.
- O. Lunov, T. Syrovets, C. Loos, J. Beil, M. Delacher, K. Tron, G. U. Nienhaus, A. Musyanovych, V. Mailänder, K. Landfester and T. Simmet, *ACS Nano*, 2011, 5, 1657-1669.
- S. Tenzer, D. Docter, J. Kuharev, A. Musyanovych, V. Fetz, R. Hecht, F. Schlenk, D. Fischer, K. Kiouptsi, C. Reinhardt, K. Landfester, H. Schild, M. Maskos, S. K. Knauer and R. H. Stauber, *Nat. Nanotechnol.*, 2013, 8, 772-781.
- M. Lundqvist, J. Stigler, G. Elia, I. Lynch, T. Cedervall and K. A. Dawson, *Proc. Natl. Acad. Sci. USA*, 2008, 105, 14265-14270.
- S. Saptarshi, A. Duschl and A. Lopata, *J. Nanobiotechnol.*, 2013, 11, 26.
- S. Fertsch-Gapp, M. Semmler-Behnke, A. Wenk and W. G. Kreyling, *Inhalation Toxicol.*, 2011, 23, 468-475.
- C. D. Walkey, J. B. Olsen, H. Guo, A. Emili and W. C. W. Chan, *J. Am. Chem. Soc.*, 2012, 134, 2139-2147.
- C. Röcker, M. Pötzl, F. Zhang, W. J. Parak and G. U. Nienhaus, *Nat. Nanotechnol.*, 2009, 4, 577-580.
- S. Tan, X. Li, Y. Guo and Z. Zhang, *Nanoscale*, 2013, 5, 860-872.
- W. Li and F. Szoka, Jr., *Pharma. Res.*, 2007, 24, 438-449.
- T. Skajaa, Y. Zhao, D. J. van den Heuvel, H. C. Gerritsen, D. P. Cormode, R. Koole, M. M. van Schooneveld, J. A. Post, E. A. Fisher, Z. A. Fayad, C. de Mello Donega, A. Meijerink and W. J. M. Mulder, *Nano Lett.*, 2010, 10, 1531-1538.
- G. U. Nienhaus, P. Maffre and K. Nienhaus, in *Methods in Enzymology*, ed. Y. T. Sergey, Academic Press, 2013, vol. Volume 519, pp. 115-137.
- O. Carion, B. Mahler, T. Pons and B. Dubertret, *Nat. Protoc.*, 2009, 2, 2383-2390.
- M. M. Markiewski, B. Nilsson, K. Nilsson Ekdahl, T. E. Mollnes and J. D. Lambris, *Trends Immunol.*, 2007, 28, 184-192.
- B. Nilsson, K. N. Ekdahl, T. E. Mollnes and J. D. Lambris, *Mol. Immunol.*, 2007, 44, 82-94.
- X. Jiang, S. Weise, M. Hafner, C. Röcker, F. Zhang, W. J. Parak and G. U. Nienhaus, *J. R. Soc. Interface*, 2010, 7, S5-S13.
- P. Maffre, K. Nienhaus, F. Amin, W. J. Parak and G. U. Nienhaus, *Beilstein J. Nanotechnol.*, 2011, 2, 374-383.
- Y. Zhang, L. Tu, Q. Zeng and X. Kong, *Chin. Sci. Bull.*, 2013, 58, 2616-2621.
- L. Shang, S. Brandholt, F. Stockmar, V. Trouillet, M. Bruns and G. U. Nienhaus, *Small*, 2012, 8, 661-665.
- B. J. C. Janssen, E. G. Huizinga, H. C. A. Raaijmakers, A. Roos, M. R. Daha, K. Nilsson-Ekdahl, B. Nilsson and P. Gros, *Nature*, 2009, 437, 505-511.
- L. Treuel, S. Brandholt, P. Maffre, S. Wiegele, L. Shang and G. U. Nienhaus, *ACS Nano*, 2014, 8, 503-513.
- L. Shang, L. Yang, J. Seiter, M. Heinle, G. Brenner-Weiss, D. Gerthsen and G. U. Nienhaus, *Adv. Mater. Interfaces*, 2014, 7, 1300079.
- C. Wilson, M. R. Wardell, K. H. Weisgraber, R. W. Mahley and I. A. Agard, *Science*, 1991, 252, 1817-1822.
- D. M. Hatters, C. A. Peters-Libeu and K. H. Weisgraber, *Trends Biochem. Sci.*, 2006, 31, 445-454.
- J. N. Adkins, *Mol. Cell. Proteomics*, 2002, 1, 947-955.
- F. Schiele, D. De Bacquer, M. Vincent-Viry, U. Beisiegel, C. Ehnholm, a. Evans, a. Kafatos, M. C. Martins, S. Sans, C. Sass, Visvikis, G. De Backer and G. Siest, *Atherosclerosis*, 2000, 152, 475-488.
- R. E. Holmlin, X. Chen, R. G. Chapman, S. Takayama and G. M. Whitesides, *Langmuir*, 2001, 17, 2841-2850.
- K. Knop, R. Hoogenboom, D. Fischer and U. S. Schubert, *Angew. Chem. Int. Ed.*, 2010, 49, 6288-6308.
- J. B. Schlenoff, *Langmuir*, 2014, 30, 9625-9636.
- P. Maffre, S. Brandholt, K. Nienhaus, L. Shang, W. J. Parak and G. U. Nienhaus, *Beilstein J. Nanotechnol.*, 2014, 5, 2036-2047.

TOC Graphics



Extremely low binding affinities of plasma proteins to MHPC lipid-enwrapped quantum dots have been revealed by fluorescence correlation spectroscopy measurements.